UCRL-JC-132377
Preprint

Defect and Dopant Diffusion in Ion Implanted Silicon: An Atomic Scale Simulation Approach

M. J. Caturla
S. K. Theiss
T. J. Lenosky
T. Diaz de la Rubia

This paper was prepared for submittal to
International Electron Devices Meeting
San Francisco, CA
December 6-9, 1998

October 15, 1998

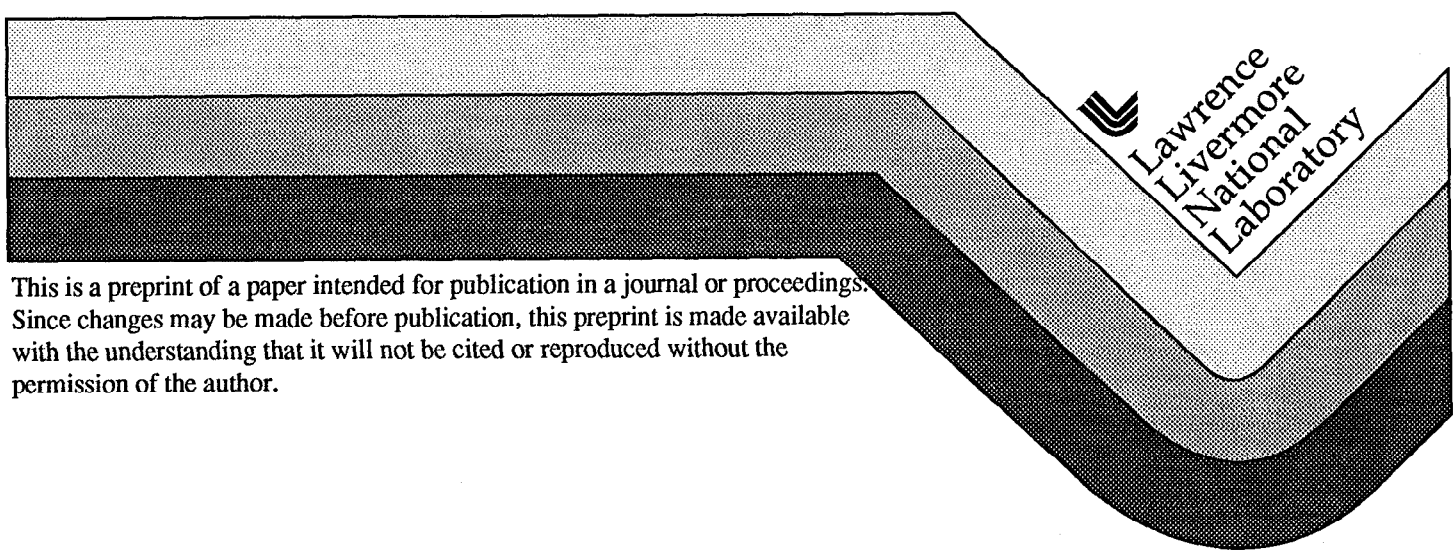

Defect and Dopant Diffusion in Ion Implanted Silicon: An Atomic Scale Simulation Approach

M.-J. Caturla, Silva K. Theiss, Thomas J. Lenosky and T. Diaz de la Rubia

Chemistry and Materials Science Directorate, Lawrence Livermore National Laboratory
Livermore, CA 94550, USA

Abstract

We present an atomistic approach to the development of predictive process simulation tools. First principles methods are used to construct a database of defect and dopant energetics. This is used as input for kinetic Monte Carlo simulations of ion implantation and dopant diffusion under a wide variety of technologically relevant conditions. Our simulations are in excellent agreement with annealing experiments on 20-80 keV B implants into Si, and with those on 50 keV Si implants into complex B-doped structures. Our calculations produce novel predictions of the time evolution of the electrically active B fraction during annealing.

Introduction

Ion implantation is currently the most widely used method for semiconductor doping, since the distribution profile of the dopants can be readily controlled. This method requires a subsequent thermal treatment of the material, in order to eliminate the damage produced during the implantation and to electrically activate the dopant atoms. During this thermal treatment, dopant atoms can diffuse. The interaction between the defects (e.g., excess interstitial Si atoms) produced during the irradiation and the dopant atoms can greatly enhance the diffusion of the dopant (e.g., B) giving diffusivity values that can be orders of magnitude larger than those at equilibrium defect concentrations. This phenomenon is known as transient enhanced diffusion (TED). So far, TED has not been a major problem in the development of semiconductor devices. However, transistors shrink from one generation to the next: gate lengths are reduced in order to improve performance. Problems arise when the gate size approaches the diffusion length of the dopant by TED. Both a fundamental understanding of TED, and the development of predictive models for the defect distribution under different annealing and implantation conditions, are necessary for the design of future devices.

Thus far, rate theory has been the most commonly used method to model the diffusion of dopants in semiconductors. However, most of these models have relied on a set of parameters that had to be fitted in order to reproduce particular experimental observations, limiting their predictive capabilities. In order to be more fully predictive, more fundamental models are necessary which include the details of the underlying physical phenomena that occur during irradiation and annealing.

The simulation of phenomena such as the diffusion of dopants requires long time scales, on the order of minutes to hours, and relatively large length scales, on the order of microns. However, during ion implantation a dopant atom deposits its energy in the crystal in just a few picoseconds. Therefore it is necessary to use a model that can link microscopic times and length scales, such as those required for defect production, with those of macroscopic phenomena, such as the dopant profile evolution. We bridge these time scales using a kinetic Monte Carlo (kMC) model, which takes as input a database of fundamental diffusion and binding energies obtained primarily by first principles approaches, and which can produce as output dopant profiles over the course of hours of annealing.

In the next section we discuss the input data necessary for such a simulation and describe the model. Subsequently the effectiveness of the model is examined for several cases of TED of B in Si. Simulations of B implantation at energies between 20 and 80 keV, and annealing temperatures between 700° and 900° C are compared to experimental data. Then Si implantation into a CVD-grown structure with a series of spikes in B concentration is simulated. Finally, the fraction of electrically active B as a function of anneal time is examined. We then conclude and discuss further work.

Method

The basic input data necessary for the simulation of dopant diffusion are migration energies and binding energies of vacancies (Vs), self-interstitials (Is) and dopants. These values can be obtained from different sources, both theoretical and, in some cases, experimental. Recent computer simulations have provided a better understanding of defect production, diffusion, and clustering in Si. V and I formation and migration energies

have been obtained using *ab initio* simulations (1-3), tight binding molecular dynamics (4) and empirical molecular dynamics (5). The interactions between dopants, impurities (e.g., C), and defects have also been studied using *ab initio* calculations. These can provide accurate information about the migration paths for dopants such as B and P, (1, 3) and about the binding energies of Vs and Is with dopant atoms (6, 7). Binding energies for I clusters and for V clusters have been obtained using Stillinger-Weber molecular dynamics and tight binding molecular dynamics models (4, 5). These energies allow the clustering of defects at different temperatures to be described.

The distribution of the dopant atoms after implantation can be accurately modeled by binary collision codes, such as UT-Marlowe (8). UT Marlowe allows simulation of different implanted species, energies, angles and doses in Si. In the binary collision approximation, two atoms interact according to a simple repulsive interatomic potential. The implanted ion undergoes a series of binary collisions with the lattice atoms. The recoiling lattice atoms collide with other lattice atoms, and so on. Thus the simulation also provides information about the cascade of defects produced by each implanted ion; that is, the location of all the Vs and Is produced during the irradiation. The defect distribution obtained from this model is valid for irradiation with light ions, when the damage is primarily in the form of V-I pairs (Frenkel pairs) and no direct amorphization is produced by the implanted ions.

Our computationally efficient kMC model is based on that of Doran and Heinisch (9). As a function of time, it tracks the locations of defects, dopants, impurities, and extended defects (clusters). These various species are all treated as point particles with basic attributes that include size and diffusivity. During the simulation the particles participate in certain events. The possible events are: the dissociation of a particle from a cluster, with rate determined by the binding energy of the cluster; the diffusive jump of a particle, where the rate depends on the migration energy; and the introduction of a new cascade, that is, a new energetic dopant and all its associated Vs and Is. The rate of cascade introduction is the dose rate of the simulated implantation. At each time step, we randomly choose among all possible events, ensuring that events occur at the proper rate by assigning each event a probability proportional to its rate. Following each chosen event, we perform all events that occur spontaneously as a result of that event. For example, an I which jumps within the capture radius of an I cluster will then spontaneously join the cluster. The simulation time is then incremented by the inverse of the sum of the rates for all possible events in the simulation box. (Thus larger time steps are used when fewer events can occur.) Because kMC focuses only on important particles and events, time scales of hours can be reached with these simulations. Clearly, care must be taken to completely enumerate the relevant particles and events.

Results

A. TED After B Implantation Into Si

Fig. 1 shows the B concentration profile for a 40 keV B implant at $2x10^{14}$ ions/cm^2, after annealing at 700° C for 240 minutes (10). The kMC results for the total B concentration profiles (circles) are compared with the secondary ion mass spectroscopy (SIMS) measurements for these conditions (solid line) (11). Similar simulations were done for energies between 20 keV and 80 keV and annealing temperatures between 700° and 900° C. Our simulations are all in good agreement with the experiments, without re-fitting of the input parameters.

One of the important features of TED profiles under the conditions described here is the presence of a fixed peak and the motion of the tail of the profile. Note that this is reproduced by our simulations. This fixed peak is due to the presence of B clusters, which are immobile. The ×s in Fig. 1 represent the concentration of B in clusters as obtained from the simulation.

From the simulations described above we have deduced the B diffusivity as a function of annealing temperature. We find $D_B = 2.2x10^{-2}$ exp (-2.7 eV/kT) cm^2/s. This is in good

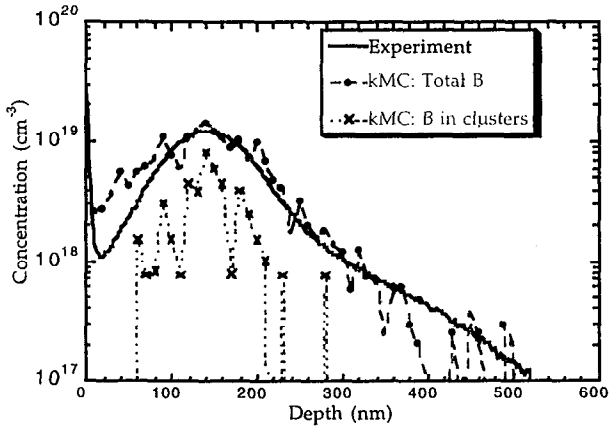

Fig. 1: Depth concentration profile for B 40 keV implantation at a dose of $2x10^{14}$ ions/cm^2 after annealing at 700°C for 240 minutes. The solid line is the SIMS measurement. The circles are the results from kMC for the total B concentration, and the ×s are the kMC values of the B concentration in B clusters.

agreement with the results of Solmi and Baruffaldi, obtained from different experimental observations: $D_B = 2.2x10^{-2}$ exp (-2.5 eV/kT) cm^2/s (12). Additionally, our simulations predict a total diffusion length, after the transient, that is lower for higher annealing temperatures. This is observed experimentally (13).

We have also calculated the B diffusivity as a function of the energy of the implant. As observed experimentally (14) there is a very small dependence of TED on implant energy. The observed differences are related to the location of the B profile with respect to the surface. At lower energies more damage is concentrated in the near-surface region, and more Is recombine at the surface rather than remaining in the bulk where they are able to induce B migration.

B. TED After Si Implantation Into B Spike Structure

The model was also tested against an extensive series of experimental studies of the diffusion of B spikes in self-implanted Si. In the experiments, several B spikes of amplitude $1x10^{19}$ cm^{-3} were grown by chemical vapor deposition (CVD). The structure was implanted with $5x10^{13}$ Si ions/cm^2 at 50 keV. Rapid thermal annealing (RTA) was performed at temperatures between 750 and 1050° C for times between 15 and 255 s (15). Fig. 2 shows the B concentration profile for the 255 s, 750° C RTA. The dotted line is the as-grown B profile, determined by SIMS. This B distribution was taken as input to the simulation. The experimental B profile after the RTA is shown by the solid line, and the simulated profile is shown by the circles and dashed line. Good agreement was also found for 15 s, 750° C and 195 s, 850° C RTAs. However, insufficient diffusion occurred in the simulation compared to the experiment at higher

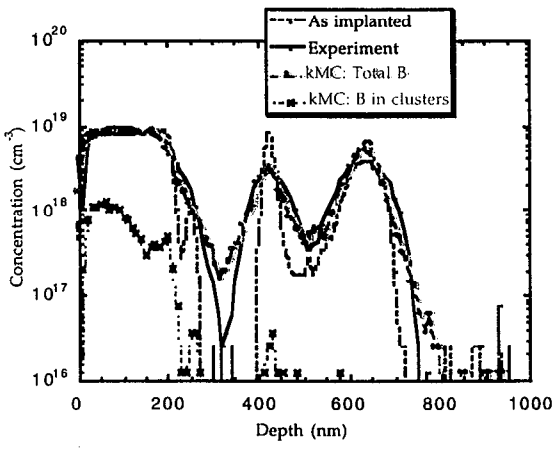

Fig. 2: B depth concentration profile after Si 50 keV implantation at a dose of $2x10^{13}$ ions/cm^2 and annealing at 750° C for 255 s. The dotted line is the B profile before annealing. The solid line is the experimental profile. Circles are the results from kMC for the total B concentration, and ×s are kMC results for B in clusters.

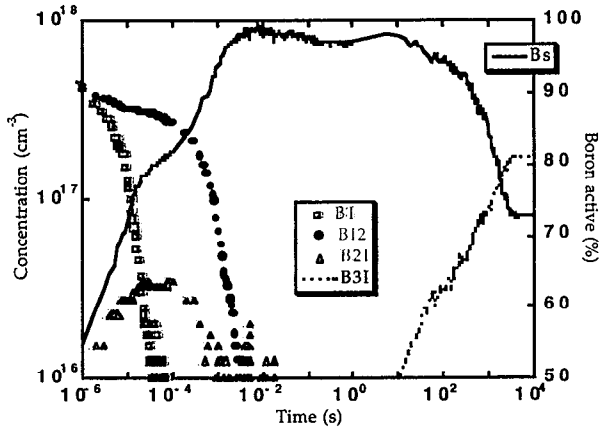

Fig. 3: kMC results for the time evolution of the substitutional and clustered B fractions following a 800° C anneal of 40 keV B-implanted Si. The percentage of B active is shown on the right ordinate, and the concentration of B-I complexes are on the left ordinate.

temperatures, suggesting that some of the energies or prefactors in the model still require fine-tuning.

C. Time Evolution of Active B Fraction

The time evolution of the populations of B-I complexes and of the fraction of electrically active (substitutional) B is shown in Fig. 3 (10). The simulation is an 800° C anneal following a 40 keV, $2x10^{14}$ ions/cm^2 B implant into Si. Remarkably, for times between 10^{-2} and 10 s, 98 % of the B is active, and the active fraction then decreases with additional annealing time. At times before 10^{-2} s, small BI, BI2, and B2I clusters which formed during the implant or very early in the annealing are present. These dissolve, mainly through interaction with the mobile vacancy flux, and leave behind substitutional B. This increases the active B fraction from 56 % immediately after implantation to 98 %. The active fraction remains constant between 10^{-2} and 10 s. After 10 s the population of B3I clusters starts to increase, and the fraction of substitutional B decreases.

We can explain this behavior by examining Fig. 4. It shows the average vacancy and interstitial cluster size as a function of time during the anneal. Also shown, on the right ordinate, is the magnitude of B TED. At early times, the defect concentration is about two orders of magnitude higher than that of B. The vacancy clusters dissolve readily at these temperatures, providing a steady supply of mobile vacancies (16). By about 10 s, however, all the vacancies have disappeared from the lattice, either through recombination with interstitials, with B-I complexes, or with the surface. Because of the sudden dearth of vacancies, three things occur: 1) a rapid increase in the average interstitial

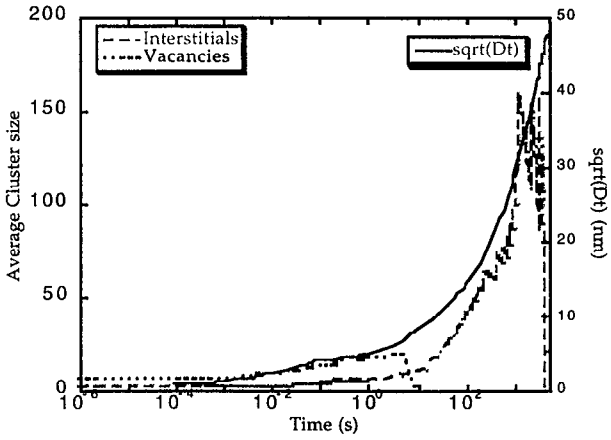

Fig. 4: Average vacancy and interstitial cluster sizes (left ordinate) and total B diffusion length (right ordinate) as a function of time during a 800° C anneal of 40 keV B-implanted Si.

cluster size, 2) an increase in the total B diffusion length, and 3) an increase in the number of B-I complexes (the B3I clusters in Fig. 3). The total B diffusion length as a function of time is plotted on the right ordinate of Fig. 4. It is interesting to note that only 4 nm of the total 48 nm B diffusion length occurs during the final interstitial cluster dissolution. During the initial 10 s, 8 nm of diffusion occurs, and 36 nm of B diffusion occurs during interstitial cluster growth.

Conclusions

We have described some recent simulations of defect and dopant diffusion using a kinetic Monte Carlo approach. Excellent agreement is found between experiments and simulations for TED at temperatures between 700° and 900° C following medium energy B implants (20 - 80 keV). Our simulations produced novel predictions of the time evolution of the electrically active B fraction during annealing, which provide an intriguing possibility for experimental verification. Good agreement was also found between experiments and simulations of TED following 50 keV Si ion implantation into CVD-grown B spike structures at temperatures up to 850° C. For anneals at 950° C and above, our simulations do not correctly predict the amount of diffusion. Additional first principles calculations are under way with the expectation that improving the accuracy of the input parameters for the initial stages of B clustering and mobile B interstitial formation will improve the results of these simulations. Another area requiring further investigation for predicting the properties of future devices is the recombination efficiency of defects and dopants at surfaces. This is a critical issue when the implantation energies are reduced, so that most of the damage is concentrated near the surface. The interactions of defects with the Si/SiO_2 interface is not fully understood, yet needs to be implemented in these kMC simulations in order to properly describe shallow junction formation. Additionally, Fermi level effects on dopant diffusion will become more important as peak dopant concentrations approach 10^{20} cm^{-3} and beyond. We are in the process of including such effects in our model.

Acknowledgments

This work was performed under the auspices of the US Department of Energy by Lawrence Livermore National Laboratory under contract W-7405-Eng-48

References

(1) C. S. Nichols, C. G. Van de Walle, S. T. Pantelides, Phys. Rev. **B40**, 5458 (1989).
(2) W.A. Harrison Mat. Res. Soc. Symp. Proc. in *Defects and Diffusion in Silicon Processing* , Vol. **469**, p. 211, Ed. T. Diaz de la Rubia, S. Coffa, P. A. Stolk, C. S. Rafferty, (1997).
(3) J. Zhu, T. Diaz de la Rubia, L. H. Yang, C. Mailhiot, G. H. Gilmer, Phys. Rev. **B54**, 4741 (1996).
(4) M. Tang, L. Colombo, J. Zhu, T. Diaz de la Rubia, Phys. Rev. **B55**, (1997).
(5) G. H. Gilmer, T. Diaz de la Rubia, D. M. Stock and M. Jaraiz, Nucl. Instrum. and Methods **B102**, 247 (1995).
(6) J. Zhu, Mat. Res. Soc. Symp. Proc. in *Defects and Diffusion in Silicon Processing* , Vol. **469**, p. 151, Ed. T. Diaz de la Rubia, S. Coffa, P. A. Stolk, C. S. Rafferty, (1997).
(7) O. Pankratov, H. Huang, T. Diaz de la Rubia, C. Mailhiot, Phys. Rev. B (1997).
(8) S. Tian, S. J. Morris, B. Obradovic, M. F. Morris, G. Wang, G. Balamurugan, A. F. Tasch, C. Snell, UT-Marlowe, Version 4.0 (1996).
(9) H. L. Heinisch, Nucl. Instrum. and Methods **B102**, 47 (1995).
(10) M.-J. Caturla, M.C. Johnson, and T. Diaz de la Rubia, Appl. Phys. Lett. **72**, 2736 (1998).
(11) A.D. Lilak, S.K. Earles, K.S. Jones, M.E. Law, International Electron Devices Meeting, IEDM Technical Digest, IEEE, Washington, DC, 1997, p.493.
(12) S. Solmi and F. Baruffaldi, J. Appl. Phys. **69**, 2135 (1991).
(13) P. A. Packan, J.D. Plummer, Appl. Phys. Lett. **56**, 1787 (1990).
(14) H.S. Chao, P. B. Griffin, J.D. Plummer, C.S. Rafferty, Appl. Phys. Lett. **69**, 2113 (1996).
(15) Ant Ural and P.B. Griffin, unpublished.
(16) P.J. Bedrossian, M.-J. Caturla, and T. Diaz de la Rubia, Appl. Phys. Lett. **70**, 176 (1997).